Digital Distortion-Free PWM and Click Modulation

Fernando Chierchie and Eduardo E. Paolini

***Abstract*—This brief exhibits the relationship between the analog click modulator, which produces a binary pulse width modulation (PWM) signal with separated baseband, and recently reported fully digital, baseband distortion-free PWM algorithms (BBDFPWM). We show that BBDFPWM not only is a discrete-time version of the click modulator but also can operate in real-time without any shortcoming of other implementations. The method can also be used for developing low distortion and efficient arbitrary signal generators. In this case, we show a procedure for the offline computation of the duty-cycles of the PWM signal with zero distortion.**

***Index Terms*—Click modulation, pulse width modulation, nonlinear distortion, baseband, power amplifiers.**

I. Introduction

PULSE width modulation (PWM) is a technique that encodes a baseband signal in the falling and/or rising edges of a pulsed signal with variable widths. It is widely used in power conversion applications [1] and switching amplifiers [2] because it allows to obtain high efficiency with transistors operating as switches rather than in its active region.

There are several practical analog and digital implementations of PWM using comparators and sawtooth or triangular carrier signals (or digital counters for digital PWM) which usually suffer from baseband distortion problems and/or require high carrier frequencies to reduce distortion [3].

A formal study of PWM is based on the representation of signals using only timing information. Some kind of bandpass signals can be represented by their zero crossings [4]. A special case is click modulation [5] which results in a binary signal that in contrast to traditional PWM modulation has zero baseband distortion. Modulation distortion is shifted to a frequency range above the band of interest using a carrier frequency that is significantly lower than that required for a conventional PWM signal with the same degree of distortion. A great effort has been made to obtain a fully-digital, real-time algorithm to implement click modulator (see [6]–[8] and references therein) but they either suffer from aliasing problems [9] or cannot be implemented in real-time.

Manuscript received May 4, 2017; accepted June 19, 2017. Date of publication June 22, 2017; date of current version March 8, 2018. This brief was recommended by Associate Editor Y. Xia. *(Corresponding author: Fernando Chierchie.)*

F. Chierchie is with the Instituto de Inv. en Ing. Eléctrica Alfredo Desages (UNS-CONICET) and Dto. de Ing. Eléctrica y de Computadoras, Universidad Nacional del Sur, Bahía Blanca 8000, Argentina (e-mail: fchierchie@uns.edu.ar).

E. E. Paolini is with the Instituto de Inv. en Ing. Eléctrica Alfredo Desages (UNS-CONICET) and Dto. de Ing. Eléctrica y de Computadoras, Universidad Nacional del Sur, Bahía Blanca 8000, Argentina, and also with the Comisión de Investigaciones Científicas, Buenos Aires, Argentina (e-mail: epaolini@uns.edu.ar).

Color versions of one or more of the figures in this paper are available online at http://ieeexplore.ieee.org.

Digital Object Identifier 10.1109/TCSII.2017.2718529

Recently, a different perspective has been explored to obtain low-carrier frequency, real-time, digital PWM with zero baseband distortion [10]–[15]. These methods compute the pulse-widths of a PWM signal based on a discrete-time input signal in such a way that the samples of the bandlimited PWM signal are equal to those of the input signal. These approaches guarantee baseband distortion-free pulse width modulation (BBDFPWM), *i.e.,* no distortion components appear in the frequency range between zero to half the PWM frequency, which can be as low as the Nyquist sampling frequency.

Previous implementations of click modulation rely on a digital version of the analog development in [5], and they cannot cope with aliasing issues produced in one of the stages of the modulator. To ameliorate this effect, large interpolation factors are required, resulting in high PWM-frequencies, losing one of the main features of click modulation that is representing a baseband signal with a minimum pulse rate. The first exact discrete-time click modulation algorithm reported in [9] suffers none of these effects, but it is not suitable for real time operation. In short, a proper discrete-time click modulator that is able to operate in real-time with reduced complexity has not been presented yet.

The contribution of this manuscript are: (1) to reveal the connection between click modulation and BBDFPWM; (2) to show that real-time implementations of BBDFPWM are the digital equivalent of click modulation: specifically we show that for affine related input signals, both methods give affine related PWM signals; (3) for arbitrary finite-length or periodic signals we develop a procedure to obtain the duty-cycles of the PWM signal with zero distortion. This was not possible with previous real-time BBDFPWM implementations (a more cumbersome method was available for discrete-time click modulation [9]).

In Section II we briefly summarize the click modulator and in Section III we review the exact BBDFPWM method. The relationship between both techniques is discussed in Section IV. The zero distortion condition of BBDFPWM is further developed in Section V. Finally in Section VI we retake the example originally proposed for click modulation [5, pp. 417–422] and show that BBDFPWM gives exactly the same duty-cycles. For completeness, simulation results showing the performance of different PWM modulations are provided.

II. Click Modulation

Click modulation [5] describes a pulse modulation technique leading to a sequence of equal-intensity Dirac impulses or "clicks" which are simply related to a leading-edge bipolar PWM signal $q(t)$ taking values $\pm\pi/2$. Given a bandlimited signal $f(t)$ which has "sufficiently small" amplitude (see Section IV-B), click modulation produces a PWM signal $q(t)$ such that $f(t)$ can be recovered free of any distortion by

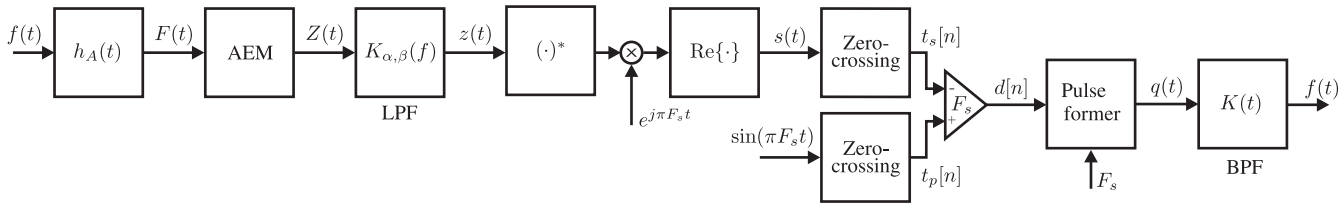

Fig. 1. Block diagram of the click modulator.

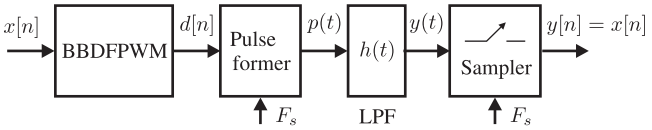

Fig. 2. Block diagram of the BBDFPWM.

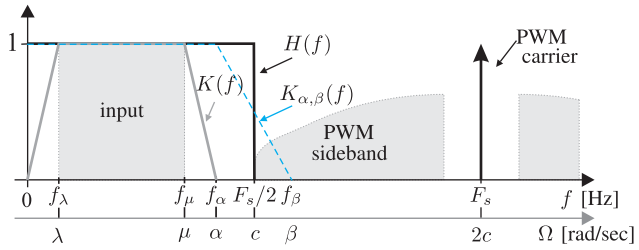

Fig. 3. Illustrative spectra. Filter characteristics of the click modulator $K(f)$ and $K_{\alpha,\beta}(f)$ and of the BBDFPWM $H(f)$.

bandpass filtering $q(t)$

$$f(t) = (K * q)(t) = \int_{-\infty}^{\infty} q(\sigma)K(t-\sigma)d\sigma$$

where $K(t)$ is the impulse response of a bandpass filter (BPF).

The leading-edge PWM signal with carrier frequency F_s can have a very small pulse rate compared to other PWM schemes. The falling edges of $q(t)$ are fixed and the raising edges are located at $t_s[n]$, the zero-crossings of a real auxiliary signal $s(t)$.

A block diagram of the click modulator is shown in Fig. 1. The auxiliary signal $s(t)$ is computed as follows. The bandlimited continuous-time input signal $f(t)$ is filtered with the analytic filter $h_A(t)$ to obtain the analytic signal $F(t) = f(t) + j\hat{f}(t)$, where $\hat{f}(t)$ is the Hilbert transform of $f(t)$. The analytic exponential modulator (AEM) gives the output $Z(t) = e^{-jF(t)}$ that has an infinite bandwidth. $Z(t)$ is filtered with $K_{\alpha,\beta}(f)$, a LPF with passband f_α and stopband f_β (see Fig. 3) to obtain $z(t)$ which is afterwards complex conjugated and modulated: $z^*(t)e^{j\pi F_s t}$. The real part of this signal is the auxiliary signal $s(t)$, *i.e.*, $s(t) = \mathrm{Re}\{z^*(t)e^{j\pi F_s t}\}$.

The clicks are located as the zeros $t_s[n]$ of $s(t)$ that verify $(n-1)T_s < t_s[n] < nT_s$ being $T_s = 1/F_s$ the PWM period. The zeros of $s(t)$ are interlaced with the zeros $t_p[n] = nT_s$ of the sinusoid $\sin(\pi F_s t)$. The normalized duty-cycles $0 \le d[n] < 1$ of the leading-edge PWM signal $q(t)$ are computed as

$$d[n] = (t_p[n] - t_s[n])/T_s = n - t_s[n]/T_s. \quad (1)$$

The derivative $f'(t)$ of the input signal $f(t)$ is

$$f'(t) = \pi \sum_{n=-\infty}^{\infty} K(t - t_s[n]) = K(t) * \pi \sum_{n=-\infty}^{\infty} \delta(t - t_s[n]), \quad (2)$$

where the last term in the convolution is the click signal. In other words, the derivative $f'(t)$ is recovered after filtering the clicks with $K(t)$.

The BPF $K(t)$ with Fourier transform $K(f)$ has corner frequencies 0, f_λ, f_μ and $f_\alpha \le F_s/2$ as shown in Fig. 3.[1] The frequency band $[f_\lambda, f_\mu]$ is the support of the input signal $f(t)$ and its derivative $f'(t)$. The band $[f_\mu, f_\alpha]$ is the guard band of the click modulator which is also free of distortion components. This band is helpful to alleviate the requirements of the low-pass filter usually used for the demodulation of the PWM signal.

III. Baseband Distortion-Free PWM

In recent years, digital, real-time PWM techniques that guarantee theoretically zero baseband distortion (negligible in actual implementations) have been presented in [10]–[15]; because of this feature we will call these methods BBDFPWM. These techniques allow to use low PWM frequency as in click modulation.

The block diagram in Fig. 2 shows the basic idea of BBDFPWM. Normalized duty-cycles $d[n]$ are derived from the input signal $x[n]$, and converted into the PWM signal $p(t)$ with carrier frequency F_s using the pulse former. To compute the duty-cycles, $p(t)$ is bandlimited to $F_s/2$ using the LPF $h(t)$ to obtain $y(t)$ and its samples $y[n]$ are taken at F_s. The duty-cycles are computed to make $y[n] = x[n]$, since $x[n]$ is bandlimited to $[0, F_s/2)$, zero baseband distortion is achieved for $p(t)$ in $[0, F_s/2)$ under the condition $y[n] = x[n]$.

We assume a discrete-time input signal $0 \le x[n] < 1$ sampled at $F_s = 1/T_s$ which is also the PWM frequency. The PWM signal $p(t) = \sum_{k=-\infty}^{\infty} p_k(t)$ is a pulse train composed of unitary-height pulses $p_k(t)$ of width $d[k]T_s$ with $0 \le d[k] < 1$ and falling edges located at kT_s. Whereas BBDFPWM can be applied to any of the well known PWM-types (leading-edge, trailing-edge and symmetric PWM [3]) we analyze leading-edge PWM to facilitate the comparison with click modulation.

The continuous-time response $y_k(t) = (p_k * h)(t)$ at the output of the ideal low-pass filter (LPF) with cutoff frequency $F_s/2$ (half the PWM frequency) and impulse response $h(t) = F_s\,\mathrm{sinc}(F_s t)$ when excited by a single "leading-edge" pulse $p_k(t) = u(t - (k - d[k])T_s) - u(t - kT_s)$ is [15]

$$y_k(t) = \int_{t-kT_s}^{t-(k-d[k])T_s} h(\tau)d\tau = R(t - (k - d[k])T_s) - R(t - kT_s)$$

where $R(t)$ is the primitive of $h(t)$ ($dR(t)/dt = h(t)$).

The output $y(t)$ produced by the filter $h(t)$ when the input is the PWM signal $p(t)$ is the sum of the outputs $y_k(t)$ produced by each of the pulses

$$y(t) = \sum_{k=-\infty}^{\infty} [R(t - (k - d[k])T_s) - R(t - kT_s)] \quad (3)$$

where $0 \le d[k] < 1$ are the duty-cycles and kT_s is the position of the falling-edges of the pulses.

[1] We follow the notation in [5] for ease of comparison.

The signal $y(t)$ is the bandlimited PWM signal, and can be sampled at F_s to obtain the discrete time-signal

$$y[n] = \sum_{k=-\infty}^{\infty} [R((n-k+d[k])T_s) - R((n-k)T_s)].$$

The goal of BBDFPWM is to determine the duty-cycles $d[n]$ from the input signal $x[n]$ such that $y[n] = x[n]$.

Solutions for this problem are developed in [11] and [12]. Approximated solutions for real-time operations were reported in [13]–[15]. Furthermore, these implementations can be tailored to reduce the approximation error to any value desired by the designer.

IV. Relationship Between Click and BBDFPWM

A. Bandpass Filter K(t), Low Pass Filter h(t) and Guard Band

Figure 3 shows the main characteristics of the spectrum of a PWM signal produced by BBDFPWM or click modulation with a carrier frequency F_s. It also depicts the BPF $K(t)$ of the click modulator which has band-pass edge frequencies f_λ and f_μ and the LPF $h(t)$ used in BBDFPWM that has a cut-off frequency $F_s/2$. Figure 3 also shows an additional x-axis with the notation defined in [5] with angular frequency units.

The guard band defined in the click modulator $[f_\mu, f_\alpha]$ is not explicitly specified for BBDFPWM but since the algorithms ensure zero distortion below $F_s/2$ the frequency band $[f_\mu, F_s/2)$ is free of any frequency component (neither from the input signal nor from the nonlinear distortion of the modulation) and can be considered as the BBDFPWM guard band.

B. Input Signal Relationship and Amplitude Restriction

For a given $f(t)$ the duty-cycles $d[n]$ or equivalently the click instants $(n-1)T_s < t_s[n] < nT_s$ are uniquely determined by the click modulator. This is because the auxiliary signal $s(t)$ has only one zero crossing in the interval $t_p[n-1] = (n-1)T_s < t < nT_s = t_p[n]$, between two zero crossings of $\sin(\pi F_s t)$, provided that the sufficiently small condition on the input signal ($|f(t)| < 1$) is honored. Under this condition it is always possible to attain a PWM with separated baseband [5].

It was recently shown [10] that to encode, without baseband distortion, a bipolar signal $-A < \hat{x}[n] < A$ bandlimited to $F_s/2$ using an unipolar "0/1" PWM signal $p(t)$ of carrier frequency F_s, the peak amplitude of the input must be less than $A = 2/\pi$. For a unipolar signal like $x[n]$ this translate into $0 < x[n] < (1+A)/2$.

Hence for a given input $|f(t)| < 1$ the discrete time signal $0 \le x[n] < (1 + 2/\pi)/2$ is obtained as

$$x[n] = x(t)|_{t=nT_s} = (1/2)(1 + (2/\pi)f(t))|_{t=nT_s}. \quad (4)$$

Defining the sampled derivative as

$$x_d[n] = T_s x'(t)|_{t=nT_s} = (T_s/\pi)f'(t)|_{t=nT_s}. \quad (5)$$

C. BBDFPWM and Click

The relationship between BBDFPWM algorithms and click modulation can be analyzed by computing the derivative $y'(t) = dy(t)/dt$ of the baseband PWM $y(t)$ in (3):

$$y'(t) = \sum_{n=-\infty}^{\infty} (h(t - nT_s + d[n]T_s) - h(t - nT_s))$$

$$= h(t) * \sum_{n=-\infty}^{\infty} \delta(t - (n - d[n])T_s) - h(t) * \sum_{n=-\infty}^{\infty} \delta(t - nT_s)$$

$$= h(t) * \sum_{n=-\infty}^{\infty} \delta(t - t_s[n]) - F_s. \quad (6)$$

The last line results from Poisson identity (see the Appendix) and replacing $t_s[n] = (n - d[n])T_s$ defined in (1). The term $(-F_s)$ removes the DC component of the impulse train. As shown in Fig. 3, the input signal has frequency support $[f_\lambda, f_\mu]$ and BBDFPWM guarantees zero distortion in $[0, F_s/2)$. Therefore, $y(t)$ and hence $y'(t)$ have no energy in the frequency intervals $[0, f_\lambda)$ and $(f_\mu, F_s/2)$. As a consequence the LPF $h(t)$ in (6) can be replaced with the bandpass filter $K(t)$ which also removes the DC component of the impulse train to obtain

$$y'(t) = K(t) * \sum_{n=-\infty}^{\infty} \delta(t - t_s[n]). \quad (7)$$

For bandpass signals the BBDFPWM criteria that imposes $y[n] = x[n]$ is equivalent to $y'(t) = x'(t)$. Replacing this equality in (7) and using (5) gives

$$K(t) * \sum_{n=-\infty}^{\infty} \delta(t - t_s[n]) = (1/\pi)f'(t),$$

and therefore solving for $f'(t)$ equals the solution (2) of the click modulator. This shows that filtering the click signal with $t_s[n]$ position determined with BBDFPWM recovers the signal $f'(t)$. Since for click modulation the $t_s[n]$ are uniquely determined for a given input signal $f(t)$ then the duty-cycles obtained with BBDFPWM are the same duty-cycles obtained with click modulation.

The PWM signal $q(t)$ obtained with click modulation is a bipolar $\pm\pi/2$ two level signal. The PWM signal $p(t)$ obtained with BBDFPWM is a unipolar signal taking values 0 and 1. Since both waveforms have the same duty cycles, they are affine related as: $p(t) = (1/2) + (1/\pi)q(t)$.

V. Zero Distortion for Periodic Inputs

In this section we develop a technique to obtain the BBDFPWM duty-cycles for periodic signals which is also applicable for finite-length signals. This case is more easily analyzed in the frequency domain. The BBDFPWM condition $y[n] = x[n]$ is recasted into the condition $y_d[n] = x_d[n]$ where $y_d[n] = T_s y'(t)|_{t=nT_s}$ is the sampled derivative of the bandlimited PWM and $x_d[n]$ the sampled derivative of the input defined in (5). In the discrete-time domain $x_d[n]$ is the signal whose DTFT is $X_d(e^{j\omega}) = j\omega X(e^{j\omega})$ for $|\omega| < \pi$ where $X(e^{j\omega})$ is the DTFT of $x[n]$. The zero distortion condition $y_d[n] = x_d[n]$ is converted into the DTFT equality

$$Y_d(e^{j\omega}) = j\omega X(e^{j\omega}), |\omega| < \pi, \quad (8)$$

where $Y_d(e^{j\omega})$ is the DTFT of $y_d[n]$. As shown in the Appendix, for $\omega \neq 0$ equation (8) can be written as

$$\sum_{n=-\infty}^{\infty} e^{-j\omega(n-d[n])} = X_d(e^{j\omega}) = j\omega X(e^{j\omega}) |\omega| < \pi. \quad (9)$$

Given $X(e^{j\omega})$, (9) should be solved for $d[n]$ to obtain zero baseband distortion. The solution exists provided that the input amplitude restriction discussed in Section IV-B is honored.

A. Zero Distortion Condition for Finite-Length or Periodic x[n]

If the input signal $x[n]$ is N-periodic or if $x[n]$ is a finite length-N signal, (9) can be recasted as a system of nonlinear equations using the discrete Fourier transform (DFT) $X[k]$ of $x[n]$ (one period if periodic). The system of equations is

$$\begin{cases} \frac{1}{N}\sum_{n=0}^{N-1} d[n] = 1/2, & k = 0, \\ \sum_{n=0}^{N-1} e^{-j\frac{2\pi}{N}k(n-d[n])} = j\frac{2\pi}{N}kX[k], & k = 1,\ldots,M \end{cases} \tag{10}$$

where $M = \lfloor N/2 \rfloor$. The first equation in (10) for $k = 0$, accounts for a mean value of $1/2$ for the normalized duty-cycles which is also the DC value of the unipolar PWM signal $p(t)$ and of $y(t)$ and $y[n]$. By taking the imaginary and real parts (10) can be reformulated into

$$\begin{cases} \frac{1}{N}\sum_{n=0}^{N-1} d[n] = 1/2, & k = 0, \\ \sum_{n=0}^{N-1} \cos\left(\frac{2\pi}{N}k(n-d[n])\right) = \frac{2\pi}{N}k\,\mathrm{Re}\{jX[k]\}, & k = 1,\ldots,M, \\ \sum_{n=0}^{N-1} \sin\left(\frac{2\pi}{N}k(n-d[n])\right) = \frac{2\pi}{N}k\,\mathrm{Im}\{jX[k]\}, & k = 1,\ldots,M. \end{cases} \tag{11}$$

Equations (10) and (11) represent a system of $2M+1$ equations in $\mathbb{R}$ with N unknowns $d[0]\cdots d[N-1]$. For N odd there are N equations with N unknowns. If $N = 2M$ is even, there are $N+1$ equation with N unknowns and one equation is discarded. In this scenario, the equations for $k = M = N/2$ are $\sin(\pi(n-d[n])) = 0$ and $\cos(\pi(n-d[n])) = 0$ since $X[N/2] = 0$ because $x[n]$ is bandlimited to $[0, F_s/2)$ or equivalently $[0, \pi)$. The $\sin(\cdot)$ equation is dropped out at the expense of possibly introducing certain distortion at $\omega = \pi$ (which corresponds to $F_s/2$) but the PWM signal is still baseband distortion-free in $[0, F_s/2)$ as expected. Alternatively the designer could drop the DC equation ($k = 0$) at the expense of possibly having a PWM signal with DC value different from $1/2$, *i.e.,* having BBDFPWM in $(0, F_s/2]$.

For the sake of brevity we don't elaborate further on the solution of this system of equations. For practical applications it can be solved by using any standard zero-finding routine.

VI. Example

We retake the example in [5, pp. 417–422] developed for click modulation and show that the duty-cycles coincide with those obtained with BBDFPWM. In the example, the PWM frequency in angular units is $2c = 5$, and $F_s = 2c/(2\pi) = 5/(2\pi)$ in Hertz. The input signal and its derivative are

$$f(t) = -(1/2)\sin(t) + (1/8)\sin(2t),$$
$$f'(t) = -(1/2)\cos(t) + (1/4)\cos(2t).$$

Comparing the maximum input frequency $2\Omega_0 = 2$ with the PWM frequency $2c$ we have: $2\Omega_0 = 2 < 2c/2 = 5/2$, which is a relatively low switching rate compared to standard PWM applications. The Hilbert transform of $f(t)$ is $\hat{f}(t) = (1/2)\cos(t) - (1/8)\cos(2t)$. Following the block diagram in Fig. 1 the output of the AEM is $Z(t) = e^{-\frac{1}{2}e^{jt} + \frac{1}{8}e^{j2t}}$. The BPF $K(t)$ defined in the example has passband edge frequencies $f_\lambda = 1/(2\pi)$ and $f_\mu = 1/\pi$. The LPF $K_{\alpha,\beta}(f)$ has frequencies $f_\alpha = 1.1/\pi$ and $f_\beta = 1.4/\pi$. The output of this LPF is $z(t) = 1 + \frac{1}{2}e^{jt}$, [5] and then

$$s(t) = \mathrm{Re}\left\{\left(1 + \tfrac{1}{2}e^{-jt}\right)e^{j\frac{5}{2}t}\right\} = \tfrac{1}{2}\cos\left(\tfrac{3}{2}t\right) + \cos\left(\tfrac{5}{2}t\right).$$

Since $f(t)$ is periodic with fundamental frequency $\Omega_0 = 1$ and the PWM frequency is $2c = 5\Omega_0$ the PWM signal $q(t)$ is periodic with 5 different duty-cycles values $d[0], d[1], d[2], d[3], d[4]$. Hence five zeros of $s(t)$ are obtained by solving

$$(1/2)\cos\left(\tfrac{3}{2}t_s[n]\right) + \cos\left(\tfrac{5}{2}t_s[n]\right) = 0 \text{ for } n = 0,\ldots,4 \tag{12}$$

knowing that $(n-1)T_s < t_s[n] < nT_s$ which gives: $t_0 = -2\arccos(\sqrt{7/8})$, $t_1 = 2\arccos(\sqrt{7/8})$, $t_2 = 2\pi/3$, $t_3 = \pi$ and $t_4 = 4\pi/3$. Using (1) the duty-cycles are

$$d[0] = (5/\pi)\arccos(\sqrt{7/8}), \quad d[1] = 1 - d[0],$$
$$d[2] = 1/3,\ d[3] = 1/2 \text{ and } \quad d[4] = 2/3. \tag{13}$$

For BBDFPWM the example proposed by Logan is reformulated using (4) and (5) into the discrete-time problem

$$x[n] = \frac{1}{2} - \frac{1}{2\pi}\sin\left(\frac{2\pi}{5}n\right) + \frac{1}{8\pi}\sin\left(\frac{4\pi}{5}n\right)$$
$$x_d[n] = -\frac{1}{5}\cos\left(\frac{2\pi}{5}n\right) + \frac{1}{10}\cos\left(\frac{4\pi}{5}n\right).$$

These are periodic signals with period $N = 5$ and hence (11) with $M = 2$ can be used to find the duty-cycles. The DFT $X_d[k]$ of one period of $x_d[n]$ gives: $X_d[0] = 0$, $X_d[1] = -1/2$, $X_d[2] = 1/4$, $X_d[3] = 1/4$, $X_d[4] = -1/2$. Only the DFT at $k = 1, 2$ is required for which $X_d[k] = j\frac{2\pi k}{N}X[k]$. Substituting these values in (11) results in

$$\begin{cases} \frac{1}{5}\sum_{n=0}^{4} d[n] = 1/2 \\ \sum_{n=0}^{4} \cos(\frac{2}{5}\pi(-n + d[n])) = -1/2 \\ \sum_{n=0}^{4} \cos(\frac{4}{5}\pi(-n + d[n])) = 1/4 \\ \sum_{n=0}^{4} \sin(\frac{2}{5}\pi(-n + d[n])) = 0 \\ \sum_{n=0}^{4} \sin(\frac{4}{5}\pi(-n + d[n])) = 0 \end{cases} \tag{14}$$

which can be solved for $0 \le d[n] < 1$, $n = 0, 1, 2, 3, 4$ using any root finding algorithm. In this case, it is easy to verify that the duty-cycles (13) found for the click modulator satisfies (14), showing that both methods result in the same duty-cycles.

A. Simulation

To emphasize advantages of click and BBDFPWM modulation over other PWM modulators a simulation of a single-leg power inverter driving a LCR load for a 1 kHz sinusoidal signal using a PWM frequency $F_s = 9$ kHz was performed. Uniform leading-edge modulation (UPWM), which is the standard digital PWM implementation, and natural leading-edge modulation (NPWM) that many discrete-time algorithms attempt to emulate were also included for comparison. Figure 4 shows the spectrum of the PWM signal for all methods. As expected, click modulation and BBDFPWM result in exactly the same spectra and both methods have zero distortion in the baseband $[0, 4.5)$ kHz. UPWM exhibits harmonics of the fundamental frequency at 2, 3 and 4 kHz. For NPWM carrier sidebands appear in baseband (usually neglected) because the frequency of the carrier is relatively low. The values of each baseband frequency component and

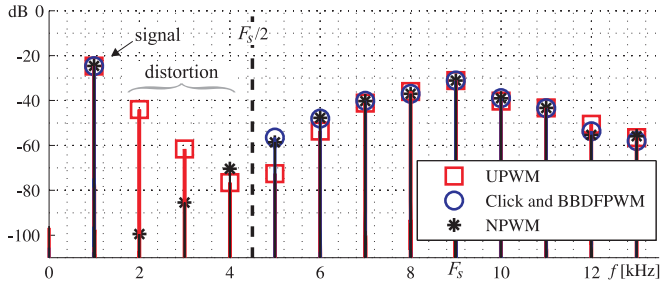

Fig. 4. PWM spectra, 1 kHz signal. PWM with $F_s = 9$ kHz.

TABLE I
AMPLITUDE OF THE BASEBAND HARMONICS

f [kHz]	BBDFPWM [dB]	click [dB]	UPWM [dB]	NPWM [dB]
1	−24.6	−24.2	−24.7	−24.6
2	0	0	−44.0	−99.5
3	0	0	−61.57	−85.5
4	0	0	−72.57	−70.4
THD %	0	0	10.91	0.52

the THD can be read from Table I. For example, the second harmonic for UPWM with amplitude −44 dB is only 19.3 dB lower than the amplitude of the fundamental component revealing the high levels of distortion introduced by UPWM. For NPWM the highest baseband harmonic is the 4-th with an amplitude 45.8 dB lower than the amplitude of the fundamental frequency.

In summary, BBDFPWM and click outperform other methods since zero baseband distortion is achieved even for very low PWM frequency.

VII. CONCLUSION

We have shown that BBDFPWM algorithm, which allows using very low switching frequency and has various fully-digital implementations can be used as a discrete-time version of the click modulator. Its advantage over click is that real-time approximate implementations can be tailored to achieve any desired distortion-level with a very low pulse rate that is not possible with reported real-time click implementations.

For any arbitrary finite length or periodic signals we also give a method to compute the zero-distortion duty-cycles that is easier than previously reported techniques.

APPENDIX
ZERO DISTORTION CONDITION IN BBDFPWM

Computing the Fourier transform of $y'(t)$ using the convolution theorem, the time-shift properties of the Fourier transform and Poisson identity results in

$$Y_d(f) = H(f)\sum_{n=-\infty}^{\infty} e^{-j2\pi\frac{f}{F_s}(n-d[n])} - \frac{H(f)}{T_s}\sum_{n=-\infty}^{\infty}\delta(f-nF_s)$$
$$= H(f)\sum_{n=-\infty}^{\infty} e^{-j2\pi\frac{f}{F_s}(n-d[n])} - F_s\delta(f) \qquad (15)$$

with $H(f)$ the Fourier transform of the LPF $h(t)$.

The derivative $y'(t)$ of the bandlimited PWM signal $y(t)$ has Fourier transform $Y_d(f)$ in (15). Since the derivative is a linear operator, $y'(t)$ is also bandlimited to $F_s/2$ and can be sampled to obtain the discrete-time signal $y_d[n] = T_s y'(t)|_{t=nT_s}$ with Discrete-Time Fourier Transform (DTFT)

$$Y_d(e^{j\omega}) = T_s F_s \sum_{k=-\infty}^{\infty} Y_d(f)|_{f=\frac{\omega F_s}{2\pi}-kF_s}.$$

Considering only one period $|\omega| < \pi$ of $Y_d(e^{j\omega})$ and using the result in (15) we have

$$Y_d(e^{j\omega}) = H\left(\tfrac{\omega F_s}{2\pi}\right)\sum_{n=-\infty}^{\infty} e^{-j\omega(n-d[n])} - 2\pi\delta(\omega)$$
$$= \sum_{n=-\infty}^{\infty} e^{-j\omega(n-d[n])} - 2\pi\delta(\omega)|\omega| < \pi \qquad (16)$$

where we applied the scaling property of the Dirac impulses and used that $H\left(\tfrac{\omega F_s}{2\pi}\right) = 1$ for $|\omega| < \pi$.

The term $2\pi\delta(\omega)$ in (16) is the DTFT of a constant of value 1 which is subtracted from the sum of exponentials to achieve zero DC level in $y_d[n]$. Substituting (16) into (8) for $\omega \neq 0$ the zero baseband distortion condition in (9) is obtained.

REFERENCES

[1] N. E. Ruger, O. Schnick, W. Mathis, and A. Mertens, "New modulation strategy with low switching frequency and minimum baseband distortion," in *Proc. Power Electron. Motion Control Conf.*, Sep. 2008, pp. 132–138.
[2] M. Streitenberger, F. Felgenhauer, H. Bresch, and W. Mathis, "Class-D audio amplifiers with separated baseband for low-power mobile applications," in *Proc. IEEE Int. Conf. Circuits Syst. Commun.*, St. Petersburg, Russia, 2002, pp. 186–189.
[3] Z. Song and D. V. Sarwate, "The frequency spectrum of pulse width modulated signals," *Signal Process.*, vol. 83, no. 10, pp. 2227–2258, Oct. 2003.
[4] R. Kumaresan and Y. Wang, "On representing signals using only timing information," *J. Acoust. Soc. America*, vol. 110, no. 5, pp. 2421–2439, 2001.
[5] B. F. Logan, Jr., "Click modulation," *AT T Bell Lab. Tech. J.*, vol. 63, no. 3, pp. 401–423, Mar. 1984.
[6] M. Streitenberger, H. Bresch, and L. Mathis, "Theory and implementation of a new type of digital power amplifier for audio applications," in *Proc. IEEE Int. Symp. Circuits Syst. (ISCAS)*, vol. 1. Geneva, Switzerland, May 2000, pp. 511–514.
[7] K. Sozanski, "Digital realization of a click modulator for an audio power amplifier," *Przeglad Elektrotechniczny*, vol. 86, no. 2, pp. 353–357, Feb. 2010.
[8] L. Stefanazzi, F. Chierchie, E. E. Paolini, and A. R. Oliva, "Low distortion switching amplifier with discrete-time click modulation," *IEEE Trans. Ind. Electron.*, vol. 61, no. 7, pp. 3511–3518, Jul. 2014.
[9] L. Stefanazzi, A. R. Oliva, and E. E. Paolini, "Alias-free digital click modulator," *IEEE Trans. Ind. Informat*, vol. 9, no. 2, pp. 1074–1083, May 2013.
[10] J. Huang, K. Padmanabhan, and O. M. Collins, "The sampling theorem with constant amplitude variable width pulses," *IEEE Trans. Circuits Syst. I, Reg. Papers*, vol. 58, no. 6, pp. 1178–1190, Jun. 2011.
[11] S. O. Aase, "A prefilter equalizer for pulse width modulation," *Signal Process.*, vol. 92, no. 10, pp. 2444–2453, Oct. 2012.
[12] F. Chierchie and E. E. Paolini, "Real-time digital PWM with zero baseband distortion and low switching frequency," *IEEE Trans. Circuits Syst. I, Reg. Papers*, vol. 60, no. 10, pp. 2752–2762, Oct. 2013.
[13] S. O. Aase, "Digital removal of pulse-width-modulation-induced distortion in class-D audio amplifiers," *IET Signal Process.*, vol. 8, no. 6, pp. 680–692, Aug. 2014.
[14] F. Chierchie, E. E. Paolini, L. Stefanazzi, and A. R. Oliva, "Simple real-time digital PWM implementation for class-D amplifiers with distortion-free baseband," *IEEE Trans. Ind. Electron*, vol. 61, no. 10, pp. 5472–5479, Oct. 2014.
[15] F. Chierchie and S. O. Aase, "Volterra models for digital PWM and their inverses," *IEEE Trans. Circuits Syst. I, Reg. Papers*, vol. 62, no. 10, pp. 2606–2616, Oct. 2015.